Contents

1 Modelling tissue self-organization: from micro to macro models 1
Pierre Degond, Diane Peurichard
1.1 Introduction 2
1.2 Individual Based Model for fibers interacting through alignment interactions 4
1.3 Derivation of a kinetic model 7
1.4 Scaling and macroscopic model 9
1.5 Conclusion 13
References 15

Index 17

Acronyms

Use the template *acronym.tex* together with the Springer document class SVMono (monograph-type books) or SVMult (edited books) to style your list(s) of abbreviations or symbols in the Springer layout.

Lists of abbreviations, symbols and the like are easily formatted with the help of the Springer-enhanced `description` environment.

IBM	Individual (agent) Based Model: microscopic model describing the evolution and interaction of each agent
ECM	Extra-Cellular Matrix

Chapter 1
Modelling tissue self-organization: from micro to macro models

Pierre Degond, Diane Peurichard

Abstract In this chapter, we present recent works concerned with the derivation of a macroscopic model for complex interconnected fiber networks from an agent-based model, with applications to, but not limited to, adipose tissue self-organization. Starting from an agent-based model for interconnected fibers interacting through alignment interactions and having the ability to create and suppress cross-links, the formal limit of large number of individuals is first investigated. It leads to a kinetic system of two equations: one for the individual fiber distribution function and one for the distribution function of connected fiber pairs. The hydrodynamic limit, in a regime of instantaneous fiber linking/unlinking then leads to a macroscopic model describing the evolution of the fiber local density and mean orientation. These works are the first attempt to derive a macroscopic model for interconnected fibers from an agent-based formulation and represent a first step towards the formulation of a large scale synthetic tissue model which will serve for the investigation of large scale effects in tissue homeostasis.

Pierre Degond
Imperial College London, London SW7 2AZ, United Kingdom, e-mail: pdegond@imperial.ac.uk

Diane Peurichard
Faculty of mathematics, Vienna University, Oskar-Morgenstern-Platz 1 1090 Wien, e-mail: diane.peurichard@univie.ac.at

This work has been supported by the "Engineering and Physical Sciences Research Council" under grant ref: EP/M006883/1 and by the National Science Foundation under NSF Grant RNMS11-07444 (KI-Net). P.D. acknowledges support from the Royal Society and the Wolfson foundation through a Royal Society Wolfson Research Merit Award. P.D. is on leave from CNRS, Institut de Mathématiques de Toulouse, France. D.P. acknowledges support by the Vienna Science and Technology Fund (WWTF) under project number LS13-029.

1.1 Introduction

Self-organization in biological systems is a process that occurs over time and leads to the spontaneous emergence of spatio-temporal structures as a result of simple interactions between agents [7]. The evolution and development of biological self-organization of systems proceeds from small, simple components that are assembled together to form larger structures that have emergent properties and behaviour, which, in turn, self-assemble into more complex structures. The latter are then maintained by a permanent turnover of different cell populations or components, which ensures the proper functioning of the tissue. Multiple evidence show that disrupting this homeostasis promotes tissue dysfunctions and diseases including cancer. Similar unbalance is a natural consequence of aging, which becomes a major problem worldwide. Understanding what factors are responsible for tissue homeostasis disruption is therefore a major issue in the science of aging. Because self-organization in biological systems involves several agents and interactions at different scales and of several types (chemical, mechanical, molecular, genomics), identifying which mechanisms are primarily involved in this organization is of tremendous difficulty. Mathematical models then provide a way of reducing the complexity of the problem, by featuring a finite set of agents and interactions that are supposed to contribute the most to the global organization of the system.

Due to their simplicity and flexibility, the most used models in the literature are Individual-Based Models (IBM), which describe the motion of each individual [1, 3, 11, 17]. An other advantage of these models is that they can incorporate any number of individual-level mechanisms. As a drawback, they are not suited to the study of large systems since the computational cost of an IBM tremendously increases with the size of the system.

The behavior of a large system of individuals can be studied through mesoscopic descriptions based on the evolution of the probability density of finding individuals in the phase space. These descriptions are usually expressed in terms of kinetic partial differential equations obtained by scaling (mean-field) limit of an IBM [18]. Finally, continuum models are proposed to describe the system at the macroscopic level. These last models describe the evolution in time of mean variables such as density, mean orientation etc. The main advantage of such models is their low computational cost. As a drawback, information on the interactions are lost at the individual level. To overcome this weakness of the macroscopic models, a possible route is to derive a macroscopic model from a microscopic one, topic which has received a lot of attention these last decades [19, 6, 16, 9]. The classical derivation consists of two steps: (i) obtain a kinetic version of the microscopic model by asymptotic limit of large number of individuals and (ii) perform the large scale limit of the kinetic model to obtain a macroscopic description .

In this chapter, we aim to apply these recent techniques to study the formation of specific structures in biological tissues. Numerous models of tis-

sue morphogenesis can be found in the literature, describing the emergence of self-organization of cells and fibers (see [20] [28] and references therein). Biological fiber networks alone have also been extensively studied in the literature. These complex networks are cross-linked dynamical plastic structures providing mechanical support to the cells and giving to the tissue the ability to change shape and adapt in response to biological and mechanical stimuli [8]. At the macroscopic level, numerous continuum models for fibrous media have also been developed in the literature. Most of them are heuristically derived from continuum theories such as [2, 27], thermodynamics [21], or viscous fluid mechanics [22]. The challenge for these models is to construct accurate constitutive laws and homogenization techniques to incorporate the dynamics of the fiber network, even if it implies a loss of information at the individual level.

The goal of this chapter is to summarize some recent works aiming at deriving a macroscopic model from an agent-based model for interconnected fibers interacting through alignment interactions first proposed in [10]. We start from an agent-based model for fibers having the ability to cross-link and unlink. Two linked fibers interact through alignment interaction at the cross link. In the asymptotic limit of a large number of individuals, we obtain a closed system of two equations describing the time evolution of the one-particle fiber distribution function and of the cross-links distribution function. The cross-links provide correlations between the fibers and consequently their distribution can be viewed as related to the two-particle fiber distribution. It is shown that the knowledge of the one-particle distributions of fibers and of cross links suffices to provide a physically relevant kinetic description of the system.

We then derive a macroscopic model by exploring the diffusion limit of the kinetic model with further scaling assumptions on the model parameters. In order to obtain a closure of the kinetic model at the level of the fiber distribution function only, we suppose that the linking/unlinking frequencies are very large: the typical linking/unlinking time is supposed to be much smaller than the typical fiber alignment time. The biological relevance of this assumption may be questioned, our main goal here is to set up a methodology which will be further refined towards providing an extensive theory of fibrous media with finite linking/unlinking times.

From these assumptions, the rescaled kinetic problem has the form of a classical diffusion approximation problem whose leading-order collision operator comes from the nematic alignment of the fibers due to the cross-links. This operator has equilibria in the form of generalized von Mises distributions of the fiber directions. Such equilibria are also observed in other systems featuring polar or nematic alignment between particles [15, 14, 4]. Therefore, the fiber distribution function is described at the macroscopic level by a fiber density and mean local orientation, raising the need for two equations providing the spatio-temporal evolution of these parameters. As there is no conservation equation other than mass conservation in the model, the con-

cept of Generalized Collision Invariants [9] is used to obtain the macroscopic system of equations for the fiber density and mean orientation. In the case of a homogeneous fiber distribution, when the density is uniform in space and constant in time, the resulting macroscopic model consists of a quasilinear parabolic equation for the fiber local mean orientation.

1.2 Individual Based Model for fibers interacting through alignment interactions

In this section, we sketch the two-dimensional agent-based model for interconnected fibers interacting through alignment interactions at the cross-links proposed in [10]. In this model, long collagen fibers are modelled as sets of segments of uniform fixed length having the ability to connect and disconnect with their intersecting neighbors. In this way, several sequentially cross-linked fiber elements model a long fiber having the ability to bend or even take possible tortuous geometries. Moreover, a link between two connected segments can be positioned at any point along this element (not only the extremities) and a given segment can be connected to any number of other segments, thereby allowing to model the branching off of a fiber into several branches. The topology of the fiber network is constantly remodelled through link creation/deletion processes, following (random) Poisson processes in time. The cross-linking process models fiber elongation and symmetrically, spontaneous unlinking of cross-linked fibers accounts for fiber breakage describing extracellular matrix (ECM) remodelling processes. We consider the following phenomena : (i) all along the link lifetime, cross-linked fibers are forced to stay linked by means of a restoring force. (ii) To model fiber resistance to bending, we suppose that pairs of linked fibers are subject to a torque that tends to align the two fibers with respect to each other. Finally, (iii) the fibers are subject to random positional and orientational noises to model the movements of the tissue and (iv) to positional and orientational potential forces, to model the action of external elements (such as cells or other tissues).

We consider a set of N fiber segments of uniform and fixed length L, each described by its center $X_i \in \mathbb{R}^2$ and its angle $\theta_i \in [-\frac{\pi}{2}, \frac{\pi}{2})$ modulo π with respect to a fixed reference direction. Each of the previously described phenomena (i-iv) is related to an energy functional, namely the energy for the maintenance of the links W_{links}, the energy for the alignment torque W_{align}, the energy for the noise contribution W_{noise} and the energy for the action of the external elements W_{ext}. The total energy is then defined as the sum of all these energies:

$$W_{\text{tot}} = W_{\text{links}} + W_{\text{align}} + W_{\text{noise}} + W_{\text{ext}}.$$

All these energies are functions of the N fiber positions $(X_i)_{i=1}^N$ and orientations $(\theta_i)_{i=1}^N$. Since W_{noise} is rather an entropy than an energy, W_{tot} is indeed the total free energy of the system. Fiber motion and rotation during a time interval between two fiber linking/unlinking events are supposed to follow the steepest descent direction of the total free energy, according to:

$$\frac{dX_i}{dt} = -\mu \nabla_{X_i} W_{\text{tot}}, \ \forall i \in \{1, \dots, N\}, \tag{1.1}$$

$$\frac{d\theta_i}{dt} = -\lambda \partial_{\theta_i} W_{\text{tot}}, \ \forall i \in \{1, \dots, N\}. \tag{1.2}$$

Eqs. (1.1) and (1.2) express the motion and rotation of the individuals in an overdamped regime in which the forces due to friction are very large compared to the inertial forces. Fiber velocity and angular speed are proportional to the force exerted on the fiber through two mobility coefficients μ and λ which are considered given.

We recall that link creation and suppresion are supposed to follow Poisson processes of frequencies ν_f and ν_d respectively. The probability that a link is created (resp. deleted) in the time interval $[t_k, t]$ is $1 - e^{-\nu_f(t-t_k)}$ (resp. $1 - e^{-\nu_d(t-t_k)}$). Given a time t at which no linking/unlinking process occurs, the set of cross-links between fibers is well defined and **supposed to have K elements**. The energies W_{links} and W_{align} of the total free energy of the system are supposed to be the sums of elementary binary potential elements computed between pairs of linked fibers, ranging over the K links of the system at time t:

$$W_{\text{links}} = \sum_{k=1}^{K} V(X_{i(k)}, \theta_{i(k)}, X_{j(k)}, \theta_{i(k)}) \tag{1.3}$$

$$W_{\text{align}} = \sum_{k=1}^{K} b(\theta_{i(k)}, \theta_{j(k)}) = \sum_{k=1}^{K} \alpha \sin^2(\theta_{i(k)} - \theta_{j(k)}). \tag{1.4}$$

The potential element V relating two linked fibers numbered $i(k)$ and $j(k)$ at their junction k is supposed to derive from a spring-like force that attracts the attachment sites of the two fibers as soon as they are displaced with respect to each other (see Fig. 1.1). The corresponding binary potential element V depends on the positions $X_{i(k)}$, $X_{j(k)}$ and orientations $\theta_{i(k)}$, $\theta_{j(k)}$ of the two linked fibers, as well as on the attachment sites $X^k_{i(k)}$, $X^k_{j(k)}$ defined by:

$$X^k_{i(k)} = X_{i(k)} + \ell^k_{i(k)} \omega_{i(k)}, \ X^k_{j(k)} = X_{j(k)} + \ell^k_{j(k)} \omega_{j(k)},$$

where $\omega_i = \omega(\theta_i) = \begin{pmatrix} \cos\theta_i \\ \sin\theta_i \end{pmatrix}$ is the unit directional vector of fiber i, $\ell^k_{i(k)} \in [-L/2, L/2]$ (resp. $\ell^k_{j(k)}$) is the algebraic distance of the attachment site of fiber $i(k)$ (resp. $j(k)$) to its center, at the time of creation of the link. We stress

out the fact that the quantities $\ell^k_{i(k)}$ and $\ell^k_{j(k)}$ remain constant throughout the link lifetime.

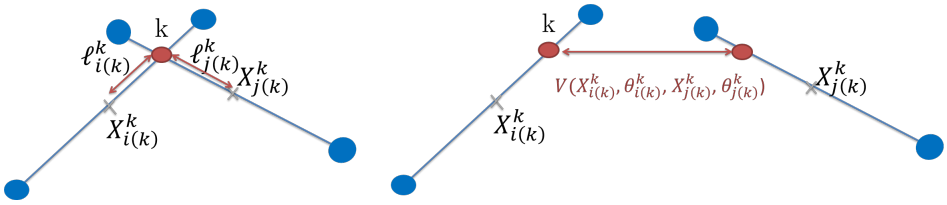

Fig. 1.1 Left: Link k connecting fibers $i(k)$ and $j(k)$. The associated link lengths $\ell_{i(k)}$ and $\ell_{j(k)}$ are indicated on the Figure. Right: restoring potential V between linked fibers $i(k)$ and $j(k)$.

The linked fiber-fiber alignment potential element b is supposed to be proportional to the square of the sine of the angle between two linked fibers $i(k), j(k)$ and only depends on the orientational angles $\theta_{i(k)}, \theta_{j(k)}$.

The external potential W_{ext} associated with the external forces is supposed to be the sum of potential forces $U(X_i, \theta_i)$ acting on each of the N fibers:

$$W_{\text{ext}} = \sum_{i=1}^{N} U(X_i, \theta_i).$$

In the case where the system describes the collagen fibers in a tissue, U aims to model the presence of cells or other organs.

We include random positional and orientational motion of the fiber elements which, in the context of biological tissues, originate from the random movements of the subject. With this aim, we introduce an entropy term:

$$W_{\text{noise}} = d \sum_{i=1}^{N} \log(\tilde{f})(X_i, \theta_i), \tag{1.5}$$

where $\tilde{f}$ is a 'regularized density' describing fibers located around point X_i and of orientation around θ_i (see [10] for details). Such an entropy term gives rise to diffusion terms at the level of the mean-field kinetic model.

In [26], simulations of this 2D microscopic model have been performed on a square domain with periodic boundary conditions, and it has been shown that Eqs. (1.1)-(1.2) correspond to a gradient descent for a quadratic penalization of a minimization problem related to the model of [25]. This last model has proved its efficiency in the modeling of complex cross-linked structures such as the ECM of adipose tissues. The study was supported by quantitative comparisons between numerical simulations and images acquired from biological experiments. From the physical point of view, phase transitions have been shown to take place when some of the model parameters are varied, namely

the fiber linking/unlinking frequencies and the cross-linked fiber alignment force. However, this model was shown to be very time-consuming for simulations at the scale of the whole tissue, raising the need for the formulation of a macroscopic level.

In the next sections, we sketch the recent results of [10] which represent a first step towards the derivation of a macroscopic model for interconnected fiber networks from its underlying microscopic model. The formal derivation consists of two main steps: (i) derivation of a kinetic model from the microscopic formulation, in the limit of a large number of fibers and cross-links and (ii) a diffusion limit of the kinetic model under appropriate scaling assumptions to obtain the macroscopic model.

1.3 Derivation of a kinetic model

In order to obtain a kinetic description of the previously described microscopic model, the empirical measure of the individual fibers, $f^N(x,\theta,t)$, is introduced:

$$f^N(x,\theta,t) = \frac{1}{N}\sum_{i=1}^{N} \delta_{(X_i(t),\theta_i(t))}(x,\theta),$$

where $\delta_{(X_i(t),\theta_i(t))}(x,\theta)$ is the Dirac delta located at $(X_i(t),\theta_i(t))$. Classically, $f^N(x,\theta,t)$ gives the probability to find a fiber within a volume dx about x with orientational angle within $d\theta$ about θ at time t. The empirical measure $g^K(x_1,\theta_1,\ell_1,x_2,\theta_2,\ell_2,t)$ of the fiber links is given by:

$$\begin{aligned} g^K = \tfrac{1}{2K}\textstyle\sum_{k=1}^{K} & \delta_{(X_{i(k)},\theta_{i(k)},\ell^k_{i(k)},X_{j(k)},\theta_{j(k)},\ell^k_{j(k)})}(x_1,\theta_1,\ell_1,x_2,\theta_2,\ell_2) \\ & +\delta_{(X_{j(k)},\theta_{j(k)},\ell^k_{j(k)},X_{i(k)},\theta_{i(k)},\ell^k_{i(k)})}(x_1,\theta_1,\ell_1,x_2,\theta_2,\ell_2), \end{aligned}$$

with a similar definition of the Dirac deltas. It gives the probability of finding a link with associated lengths within a volume $d\ell_1 d\ell_2$ about ℓ_1 and ℓ_2, this link connecting a fiber located within a volume $dx_1\frac{d\theta_1}{\pi}$ about (x_1,θ_1) with a fiber located within a volume $dx_2\frac{d\theta_2}{\pi}$ about (x_2,θ_2). One notes that (ℓ_1,ℓ_2) is defined in $[-\frac{L}{2},\frac{L}{2}]^2$. Then, at the limit $N,K\to\infty$, $\frac{K}{N}\to\xi$, where $\xi>0$ is a fixed parameter, $f^N\to f$, $g^K\to g$ where f and g satisfy the equations given in the following theorem (see [26]):

Theorem 1.1. *The formal limit of Eqs.* (1.1), (1.2) *for* $K,N\to\infty$, $\frac{K}{N}\to\xi$, *where* $\xi>0$ *is a fixed parameter reads:*

$$\frac{\partial f}{\partial t} - \mu\Big(\nabla_x\cdot((\nabla_x U)f) + \xi\nabla_x\cdot F_1 + d\Delta_x f\Big) - \lambda\Big(\partial_\theta((\partial_\theta U)f) + \xi\partial_\theta F_2 + d\partial_\theta^2 f\Big) = 0, \tag{1.6}$$

and

$$
\begin{aligned}
\frac{\partial g}{\partial t} &-\mu\Big(\nabla_{x_1}\cdot\big(g\nabla_x U(x_1,\theta_1)+\xi\frac{g}{f(x_1,\theta_1)}F_1(x_1,\theta_1)\big)\\
&+\nabla_{x_2}\cdot\big(g\nabla_x U(x_2,\theta_2)+\xi\frac{g}{f(x_2,\theta_2)}F_1(x_2,\theta_2)\big)\\
&+d\nabla_{x_1}\cdot(\frac{g}{f(x_1,\theta_1)}\nabla_x f(x_1,\theta_1))+d\nabla_{x_2}\cdot(\frac{g}{f(x_2,\theta_2)}\nabla_x f(x_2,\theta_2))\Big)\\
&-\lambda\Big(\partial_{\theta_1}\big(g\partial_\theta U(x_1,\theta_1)+\xi\frac{g}{f(x_1,\theta_1)}F_2(x_1,\theta_1)\big)\\
&+\partial_{\theta_2}\big(g\partial_\theta U(x_2,\theta_2)+\xi\frac{g}{f(x_2,\theta_2)}F_2(x_2,\theta_2)\big)\\
&+d\partial_{\theta_1}(\frac{g}{f(x_1,\theta_1)}\partial_\theta f(x_1,\theta_1))+d\partial_{\theta_2}(\frac{g}{f(x_2,\theta_2)}\partial_\theta f(x_2,\theta_2))\Big)=S(g),
\end{aligned}
\tag{1.7}
$$

where

$$
\begin{aligned}
F_1(x_1,\theta_1) &= \textstyle\int(g\nabla_{x_1}V)(x_1,\theta_1,\ell_1,x_2,\theta_2,\ell_2)d\ell_1 d\ell_2\frac{d\theta_2}{\pi}dx_2,\\
F_2(x_1,\theta_1) &= \textstyle\int\big(g(\partial_{\theta_1}V+\partial_{\theta_1}b)\big)(x_1,\theta_1,\ell_1,x_2,\theta_2,\ell_2)d\ell_1 d\ell_2\frac{d\theta_2}{\pi}dx_2,
\end{aligned}
$$

and $S(g)$ is given by:

$$
S(g)=\nu_f f(x_1,\theta_1)f(x_2,\theta_2)\delta_{\bar\ell(x_1,\theta_1,x_2,\theta_2)}(\ell_1)\delta_{\bar\ell(x_2,\theta_2,x_1,\theta_1)}(\ell_2)-\nu_d g, \tag{1.8}
$$

where $\delta_{\bar\ell}(\ell_1)$ denotes the Dirac delta at $\bar\ell$, i.e. the distribution acting on test functions $\phi(\ell_1)$ such that $\langle\delta_{\bar\ell}(\ell_1),\phi(\ell_1)\rangle=\phi(\bar\ell)$

This kinetic model consists of two evolution equations. Eq. (1.6) is an equation for the individual fibers and describes the evolution of the one-particle distribution function f. Eq. (1.7) is an equation for the links between fiber pairs, where g describes the cross-link distribution function. It can be related to the two-particle fiber distribution function. As the links are tightly tied to the fibers, they are convected by them and follow their motion. Simultaneously, they constrain the linked fibers to move together, so they directly influence their motion. The action of the links on the individual fiber motion is contained in the force terms F_1 and F_2 of Eq. (1.6) where V is the restoring potential which forces cross-linked fibers to stay connected (contained in the term W_{links} of the microscopic model). The second and fifth terms of Eq. (1.6) describe transport in physical and orientational spaces due to the external potential U (contained in the potential W_{ext} of the microscopic model). The kinetic counterpart of the alignment force between linked fibers (contained in the term W_{align} of the microscopic model) is encompassed in the second term of the force F_2 and only acts on the orientation of the fibers. The fourth and seventh terms of Eq. (1.6) are diffusion terms of amplitude λd and μd respectively. They represent the random motion of the fibers and originate from the interactions described in W_{noise} of the microscopic model. The individual motion of the fibers is thus related to the motion of their

linked neighbors. The left-hand side of Eq. (1.7) describes the evolution of the links between fibers. It is composed of the convective terms generated by the external potential and by the diffusion terms. The forces induced by the restoring potential generated by the links again give rise to the nonlocal terms F_1 and the first term of F_2. The right hand side $S(g)$ of Eq. (1.7) results from the Poisson processes of linking/unlinking intersecting fibers at frequencies ν_f and ν_d, respectively. The first term of Eq. (1.8) describes the formation of the link and the Dirac deltas indicate that, at the link creation time, the link lengths ℓ_1 and ℓ_2 (in $[-L/2, L/2]$) are set by the geometric configuration of the intersecting fibers at the attachment time. The second term describes fiber unlinking at the rate set by the Poisson process, i.e. ν_d.

The rigorous proof of the convergence of the microscopic model to the kinetic model is still an open question, and this derivation still needs validation through theoretical analysis and numerical simulations. However, this model is to our knowledge a unique explicit example of a kinetic model written in terms of the one and two particle distribution functions and closed at this level. Moreover, the distribution function g can be seen as a way of describing the random graph of the fiber links, a description which could be useful to describe other kinds of random networks. In the sequel, the diffusion limit of this kinetic model is performed via rescaling of space and time, and introducing scaling assumptions on the model parameters.

1.4 Scaling and macroscopic model

In order to perform a diffusion limit of the kinetic model of the previous section, we introduce a small parameter $\varepsilon \ll 1$ and set $\tilde{x} = \sqrt{\varepsilon}x$ and $\tilde{t} = \varepsilon t$. This leads to $\tilde{\ell} = \sqrt{\varepsilon}\ell$, $\tilde{f}(\bar{x}, \theta) = \varepsilon^{-1} f(x, \theta)$ and $\tilde{g}(\tilde{x}_1, \theta_1, \tilde{\ell}_1, \tilde{x}_2, \theta_2, \tilde{\ell}_2) = \varepsilon^{-3} g(x_1, \theta_1, \ell_1, x_2, \theta_2, \ell_2)$. We then introduce the following scaling hypothesis on the model parameters: We suppose that the external potential $U(x, \theta)$ is decomposed into $U(x, \theta) = U^0(x) + U^1(\theta)$, where U^0 is acting on the space variable only and U^1 is a π-periodic potential only acting on the fiber orientation angles. The external potential acting on the space variables is supposed to be one order of magnitude stronger than the one acting on the fiber rotations: $U^0 = O(1)$, $U^1 = O(\varepsilon)$. The strength of the alignment potential is supposed to be (large) of order $O(\varepsilon^{-1})$. The intensity of the alignment potential between linked fibers is supposed to be (small) of order $O(\varepsilon)$, and the diffusion coefficient and parameter ξ (ratio between the total number of fibers and total number of links) are supposed to stay of order 1. The main assumption in this scaling, which is introduced to simplify the analysis of the system, consists in supposing that the processes of linking and unlinking occur at a very fast time scale, i.e. $\nu_f, \nu_d = O(\frac{1}{\varepsilon^2})$.

It is noteworthy that these scaling hypothesis are done for technical reasons, and in this regime it has first been shown (see [10]) that the two particle

distribution function g reduces to:

$$g^\varepsilon(x_1,\theta_1,\ell_1,x_2,\theta_2,\ell_2) = \frac{\nu_f}{\nu_d} f^\varepsilon(x_1,\theta_1) f^\varepsilon(x_2,\theta_2) \delta_{\bar{\ell}(x_1,\theta_1,x_2,\theta_2)}(\ell_1)\ \delta_{\bar{\ell}(x_2,\theta_2,x_1,\theta_1)}(\ell_2) + O(\varepsilon^2).$$

Note that as $\varepsilon \to 0$, the correlations built by the fiber links disappear since the two-particle distribution function then corresponds to the product of two one-particle distribution functions. This property comes from the fact that in this scaling limit, links appear and disappear almost instantaneously, making the timescale of the action of the restoring force much longer than the lifetime of a link.

Moreover, in this scaling limit, it can be shown that the one particle distribution function f^ε formally satisfies (neglecting the terms in $O(\varepsilon^2)$, see [10]):

$$\varepsilon\left[\partial_t f^\varepsilon - \partial_\theta\left(\left[\partial_\theta U^1 + \xi G[f^\varepsilon](x,\theta)\right] f^\varepsilon\right) - \mu d \Delta_x f^\varepsilon\right] = Q(f^\varepsilon), \tag{1.9}$$

where $Q(f)$ is the following collision operator:

$$Q(f) = d\partial_\theta^2 f + \xi \partial_\theta(\partial_\theta \Phi[f] f), \tag{1.10}$$

and

$$\Phi[f^\varepsilon](x_1,\theta_1) = C_1 \int_{-\frac{\pi}{2}}^{\frac{\pi}{2}} \sin^2(\theta-\theta_2) f^\varepsilon(x_1,\theta_2) \frac{d\theta_2}{\pi} \tag{1.11}$$

$$G[f^\varepsilon](x_1,\theta_1) = C_2 \sum_{i,j=1}^{2} \frac{\partial^2}{\partial x_i \partial x_j} \int_{-\frac{\pi}{2}}^{\frac{\pi}{2}} f^\varepsilon(x_1,\theta_2) B_{ij}(\theta_1,\theta_2) \frac{d\theta_2}{\pi}, \tag{1.12}$$

$$C_1 = \frac{\alpha L^2 \nu_f}{2\nu_d}\ ,\ C_2 = \frac{\alpha L^4 \nu_f}{48 \nu_d}, \tag{1.13}$$

with α the alignment force intensity (see Eq. 1.4). Finally,

$$B(\theta_1,\theta_2) = \sin 2(\theta_1-\theta_2)[\omega(\theta_1)\otimes\omega(\theta_1) + \omega(\theta_2)\otimes\omega(\theta_2)] = \big(B_{ij}(\theta_1,\theta_2)\big)_{i,j=1,2}, \tag{1.14}$$

where $A\otimes B$ is the tensor product between vectors A and B: $(A\otimes B)_{ij} = A_i B_j$. Eq. (1.9) shows that the interactions at leading order are contained in the so-called collision operator $Q(f)$ (Eq. (1.10)), which expresses that the alignment potential (contained in the functional $\Phi[f](x,\theta)$) is counter-balanced by the diffusion term which tends to spread the particles isotropically on the sphere. It is noteworthy that the alignment force is local in space and consists of a sum of elementary alignment forces generated by intersecting fibers. The other terms (left-hand side of Eq (1.9)) act at lower order ε and contain

the contribution of the external potential in orientation, the next order contribution of the alignment force between linked fibers (term $G[f]$) and the diffusion in space (due to fiber random motion in the microscopic model).

We now aim to study the limit $\varepsilon \to 0$ in Eq (1.9). Formally, if we let $f^\varepsilon \to f$, as $Q(f^\varepsilon) = O(\varepsilon)$, we have $Q(f) = 0$. Therefore, f is an equilibrium of the collision operator, and consists of a Von Mises distribution $f(x, \theta, t)$ (see [10]):

$$f(x,\theta,t) = \rho(x,t) M_{\theta_0(x,t)}(\theta)$$
$$M_{\theta_0(x,t)}(\theta) = \frac{e^{r\cos 2(\theta-\theta_0(x,t))}}{\displaystyle\int_{-\frac{\pi}{2}}^{\frac{\pi}{2}} e^{r\cos 2\theta}\frac{d\theta}{\pi}},$$

where $\rho(x,t)$ is the fiber density, $\theta_0(x,t)$ the fiber local orientation and r the order parameter given by:

$$r = \frac{\xi\alpha L^2 \rho(x,t) c(r) \nu_f}{4 d \nu_d}, \qquad c(r) = \int_{-\frac{\pi}{2}}^{\frac{\pi}{2}} \cos 2\theta M_0(\theta)\frac{d\theta}{\pi}.$$

Note that $c(r)$ does not depend on θ_0. Therefore in the limit $\varepsilon \to 0$, the one particle distribution function is fully described by the density $\rho(x,t)$ and the mean local orientation $\theta_0(x,t)$. Therefore, we need to find two equations to determine $\rho(x,t)$ and $\theta_0(x,t)$. Let us note that the local fiber number is the only quantity conserved by the interactions. In particular, there is no momentum conservation. Therefore, the only collision invariants of the collision operator are the constants. The integration of Eq. (1.9) against these invariants does not allow us to find the evolution equation for the mean orientation. In order to obtain an equation for θ_0, inspired from [9], the concept of Generalized Collision Invariants (GCI), i.e. of collision invariants when acting on a restricted subset of functions f, is used. Thanks to this new concept and in the case of a homogeneous fiber distribution $\rho(x,t) = \rho_0$ (see [10]), the local fiber orientation $\theta_0(x,t)$ solves:

$$\partial_t \theta_0 - \sum_{i,j=1}^{2} \partial_{x_i}\big(a_{ij}(\theta_0)\partial_{x_j}\theta_0\big) + \alpha_5 h(\theta_0) = 0, \tag{1.15}$$

where $a_{ij} \in \mathbb{R}$ for $i,j = 1,2$ are the coefficients of a 2×2 matrix A such that:

$$A(\theta) = \begin{pmatrix} \alpha_2 - \alpha_3\cos 2\theta & -\alpha_3 \sin 2\theta \\ -\alpha_3 \sin 2\theta & \alpha_2 + \alpha_3 \cos 2\theta \end{pmatrix}. \tag{1.16}$$

The coefficients $\alpha_1, \alpha_2, \alpha_3$ and α_5 are fully determined by the parameters r, d and L. Their expression is omitted here for the sake of simplicity (see [10]). Finally, the function h is the macroscopic counterpart of the external potential U and reads:

$$h(\theta_0) = \int_{-\frac{\pi}{2}}^{\frac{\pi}{2}} U'(\theta) M_{\theta_0}(\theta) \frac{d\theta}{\pi}. \tag{1.17}$$

In [26] it has been shown that, in the stationary case, Eq. (1.15) is a quasi-linear elliptic equation, and the existence of solutions was proven under stuctural conditions for the external potential $h(\theta_0)$.

Numerical simulations of the stationary solutions of Eq. (1.15) on a 2D square domain with Dirichlet boundary conditions have been performed in [26]. For an external rotation potential U forcing the fibers to reach orientation $\pm\frac{\pi}{2}$, the fiber network could be seen as a continuum medium subjected to compressive stress. In this case, a buckling phenomenon was observed, corresponding to an instability characterized by a sudden sideways failure of the structure subjected to high compression. The boundary conditions determined the mode of bending, the load corresponded to the external potential force and the point of failure depended on the elastic modulus of the fiber network contained in parameter α_3. In Fig. 1.2, we show an example of simulation obtained for the following external force:

$$U(\theta) = c_u \sin^2(\theta - \frac{\pi}{2}),$$

where c_u is the intensity of the force. We consider a 2D square domain $[-0.5, 0.5] \times [-0.5, 0.5]$ with Dirichlet boundary conditions on the left and right sides of the domain ($\theta = 0.98\frac{\pi}{4}$ and $\theta = -\frac{\pi}{4}$ respectively), and periodic boundary conditions on the top and bottom. Details on the numerical method can be found in [26]. In this setting, we can show that the solution θ does not depend on the y-direction and we plot in Fig. 1.2 the fiber orientation as function of x for $y = 0.2$, for four different values of the external potential intensity c_u.

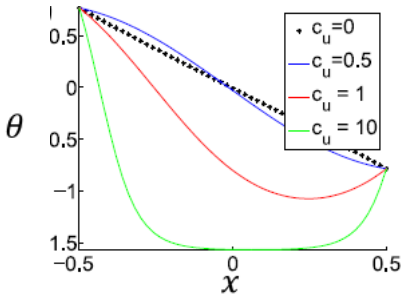

Fig. 1.2 Fiber orientation as function of x for four different values of the external potential c_u: $c_u = 0$ (black dots), $c_u = 0.5$ (blue curve), $c_u = 1$ (red curve) and $c_u = 10$ (green curve). Boundary conditions $\theta(-0.5, y) = 0.98\frac{\pi}{4}$ and $\theta(0.5, y) = -\frac{\pi}{4}$ for all $y \in [-0.5, 0.5]$.

As shown by Fig. 1.2, two stationary states are obtained when introducing the rotation potential: (i) a symmetric state with respect to the x-direction (black dots and blue curve), and (ii) an asymmetric state in which all the fibers are oriented in $-\frac{\pi}{2}$ (red curve). There exists a critical c_u for which the solutions are in the unstable configuration: a slight increase of c_u leads the solution to buckle and change for configuration (ii). These simulations highlight the physical relevance of the macroscopic model to describe interconnected networks as elastic materials with internal resistance depending on the density of the fiber links.

Moreover, numerical simulations showed a very good agreement between the macroscopic model and the microscopic formulation in a well chosen regime of fiber linking/unlinking. We illustrate this in Fig. 1.3, where we show simulations of the microscopic model given by Eqs. (1.1)-(1.2) rescaled with the scaling of section 1.4 with $\varepsilon = \frac{1}{4}$, and small linking/unlinking ratio $\frac{\nu_f}{\nu_d} = 0.1$. Figs. 1.3 (A1) to (A3) show simulations for increasing values of the noise d: $d = 10^{-4}$, $d = 10^{-3}$ and $d = 5.10^{-3}$, and external potential $c_u = 0.01$. In Fig. 1.3 (B) we present the simulations for $c_u = 0.1$. For each, we show the microscopic simulation at equilibrium, and we plot the profiles of θ as function of x, averaged over the y-direction. Black curves correspond to the solutions of the microscopic model, red curves are the profiles of the solutions of the macroscopic one. For small d and small external potential $c_u = 0.01$ (A1,A2), fibers are oriented towards $\pm\frac{\pi}{2}$ on the left and right hand sides of the domain, with a zone of fibers horizontally oriented in the center, as predicted by the macroscopic model. For increasing d (A3), the fibers are disorganized and have mean orientation $\pm\frac{\pi}{2}$. The macroscopic model captures the same features for the same parameters.

As depicted in Fig. 1.3, we obtain a very good agreement between the microscopic and macroscopic simulations for a small linking/unlinking ratio.

However, it was shown that the fiber links density has a strong impact on the final structures obtained by the microscopic model that the macroscopic model does not capture. This is due to the fact that the scaling supposes that the linking/unlinking process is quasi instantaneous. This assumption makes the action of the links vanish in the macroscopic model, and no memory effect of the fiber cross-links remains. Works are in progress to better account for these effects in the macroscopic model.

These simulations are a first step towards the validation of the macroscopic model for interconnected fibers and its derivation from a microscopic description. In conclusion, we give some exciting perspectives of this study.

1.5 Conclusion

The works presented in this chapter are, to our knowledge, the first attempt to derive as rigorously as possible a macroscopic model for temporarily cross-

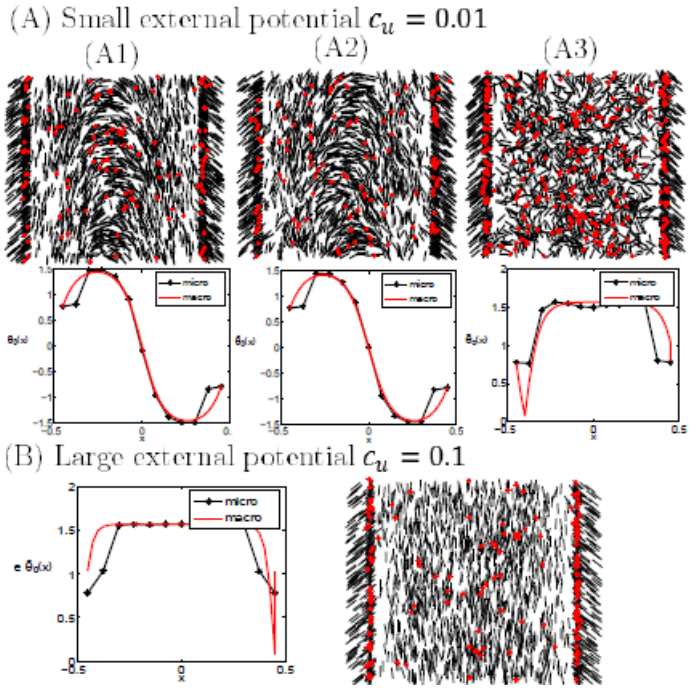

Fig. 1.3 Simulations of the microscopic model with external potential $c_u = 0.01$ and ratio $\xi = 0.1$. From A1 to A3: for increasing values of the noise d: $d = 10^{-4}$, $d = 10^{-3}$ and $d = 5.10^{-3}$. First line: simulation at equilibrium, second line: profiles of the solutions to the microscopic model averaged over the y-direction and over 10 simulations (black curves), and profiles of the solutions to the macroscopic model (red curves). For small d and small external potential $c_u = 0.01$ (A1,A2), fibers are oriented towards $\pm\frac{\pi}{2}$ on the left and right hand sides of the domain, with a zone of fibers horizontally oriented in the center, as predicted by the macroscopic model. For increasing d (A3), the fibers are disorganized and have mean orientation $\pm\frac{\pi}{2}$. The macroscopic model captures the same features for the same parameters. (B) Case $c_u = 0.1$ and $d = 10^{-3}$. In this case, all the fibers reach orientation $\pm\frac{\pi}{2}$ due to the large intensity of the external potential for both models.

linked fibers interacting through alignment at their links from a microscopic model. The kinetic model obtained in the limit of a large number of individuals of the microscopic model involves two distribution functions: the fiber distribution function and the cross-link distribution function, and is closed at the level of the two-particle distribution function. The diffusive limit of the kinetic model in the regime of instantaneous fiber linking/unlinking leads to a system of two coupled nonlinear diffusion equations for the fiber density and mean orientation. In the homogeneous density case, physical properties of the solutions of the macroscopic model have been observed and the numerical comparison between the macroscopic model and the microscopic one has shown the relevance of the model in an appropriately chosen fiber linking/unlinking regime.

These works present numerous exciting perspectives in the mathematical and biological fields. Mathematically, rigorously proving the convergence of the particle model towards the mean-field limit or proving existence and uniqueness of smooth solutions for the macroscopic diffusion system with non-homogeneous fiber density are immediate perspectives. In the latter case, the much more complex system of two coupled highly non linear equations - for fiber density and local mean orientation - requires the development of advanced numerical methods. Further perspectives on this model include numerical simulations of the complete kinetic model and comparisons with the microscopic formulation. Finally, the establishment of a hydrodynamic scaling based on a more realistic assumption for fiber linking/unlinking dynamics would enable to understand how the presence of fiber links affects the macroscopic dynamics.

From the biological viewpoint and in the long-term, the hope is to couple the macroscopic model for fiber networks with a macroscopic model for the cells. The resulting coupled model will provide a complete "synthetic tissue" model, i.e. a large scale counterpart of the agent-based tissue model described in [25]. It will serve for the investigation of large scale effects in general tissue homeostasis. Obviously, biological relevance will require to extend the models to three spatial dimensions. As the present derivation could be extended to the 3D case without further complications, the main challenge lies in the modelling of the fibers and the links. For fibers, one could consider ellipsoids and further development is needed for the fiber links, which would lead to a different source term in the macroscopic model.

References

1. Alonso, R., Young, J., Cheng, Y.: *A particle interaction model for the simulation of biological, cross-linked fibers inspired from flocking theory*, Cell. mol. bioeng., 7(1):58-72 (2014)
2. Alt, W., Dembo, M.: Cytoplasm dynamics and cell motion: two phase flow models, *Math. Biosci.* **156** 207-228 (1999)
3. Astrom, J.A., Kumar, P.B.S., Vattulaine, I., Karttunen, M.: *Strain hardening in dense actin networks*, Phy. Rev. E. 71:050901 (2005)
4. Baskaran, A., Marchetti, M. C.: Hydrodynamics of self-propelled hard rods, Phys. Rev. E 77 011920 (2008)
5. Hwang M., Garbey M., Berceli S.A., Tran-Son-Tay R.: Rule-Based Simulation of Multi-Cellular Biological Systems-A Review of Modeling Techniques, Cell Mol Bioeng 2(3):285-294 (2009)
6. Bertin, E., Droz, M., Gregoire, G.: Hydrodynamic equations for self-propelled particles: microscopic derivation, stability analysis, J. Phys A: Math. Theor. 42, 445001 (2009)
7. Camazine, S., Deneubourg, J.L., Franks, N.R., Sneyd, J., Theraulaz, G., Bonabeau, E.: Self-Organization in Biological Systems. Princeton, New Jersey: Princeton University Press (2001)
8. O. Chaudury, O., Parekh, S. H., Fletcher, D.A.: Reversible stress softening of actin networks, 910 Nature, 445:295-298 (2007)

9. Degond, P., Motsch, S.: Continuum limit of self-driven particles with orientation interaction, Math. Mod. Meth. App. S. 18:1193-1215 (2008)
10. Degond, P., Delebecque, F., Peurichard, D.: Continuum model for linked fibers with alignment interactions, Math. Mod. Meth. App. S. 26:269-318 (2016)
11. DiDonna, B.A., Levine A.J.:*Filamin cross-linked semiflexible networks: Fragility under strain*, Phys Rev Lett. 97(6):068104 (2006)
12. Divoux A., Clement K.: Architecture and the extracellular matrix: the still unappreciated components of the adipose tissue. Obes Rev 12:494-503 (2011)
13. Drasdo D.: On selected individual-based approaches to the dynamics in multicellular systems. Multiscale Modelling and Numerical Simulations, eds W. Alt, M. Chaplain, M. Griebel, J. Lenz (Birkhauser, Basel, Switzerland), pp 587 109-203 (2003)
14. Frouvelle, A.: A continuum model for alignment of self-propelled particles with anisotropy and density-dependent parameters, Math. Models Methods Appl. Sci. 22 1250011 (2012)
15. Ginelli, F., Peruani, F., Bär, M., Chaté, H.: Large-scale collective properties of self-propelled rods, Phys. Rev. Lett. 104 184502 (2010)
16. Ha, S.Y. Tadmor, E.: From particle to kinetic, hydrodynamic descriptions of flocking, Kinetic, Related Models, 1:415-435 (2008)
17. Head, D. Levine, A.J., MacKintosh,F.C: *Distinct regimes of elastic response, deformation modes of cross-linked cytoskeletal, semiflexible polymer networks*, Phys. Rev. E. 68:061907 (2003)
18. Hillen, T.: M5 mesoscopic and macroscopic models for mesenchymal motion, J. Math. 960 Biol. 53:585-616 (2006)
19. Engwer, C., Hillen, T., Knappitsch, M., Surulescu, C.: Glioma follow white matter tracts: a multiscale DTI-based model, J. Math. Biol 71(3):551-82 (2015)
20. Ilina, O., Friedl,P.: Mechanisms of collective cell migration at a glance, J. Cell Sci. 122:3203-3208 (2009)
21. Joanny, J. F., Jülicher, F., Kruse, K., Prost, J.: Hydrodynamic theory for multicomponent active polar gels, *New J. Phys.* **9** 422 (2007)
22. Karsher, H., Lammerding, J., Huang, H., Lee, R. T., Kamm, R. D., Kaazempur-Mofrad, M. R. : A three-dimensional viscoelastic model for cell deformation with experimental verification, *Biophysical Journal* **85** 3336-3349 (2003)
23. Napolitano, L.: The differentiation of white adipose cells an electron microscope study. J Cell Biol 18:663-679 (1963)
24. Ouchi, N., Parker J.L., Lugus J.J. and Walsh, K. :, Adipokines in inflammation and metabolic disease. Nat Rev Immunol 11:85-97 (2011)
25. Peurichard, D. et al.: Simple mechanical cues could explain adipose tissue morphology, submitted
26. Peurichard, D.: Macroscopic model for linked fibers with alignment interactions: existence theory and numerical simulations, to appear in SIAM MMS
27. Taber, L. A., Shi, Y., Yang, L., Bayly, P. V.: A poroelastic model for cell crawling including mechanical coupling between cytoskeletal contraction and actin polymerization, *Journal of Mechanics of Materials and Structures* **6** 569-589 (2011)
28. Vicsek, T., Zafeiris, A.: Collective motion, Phys. Rep. 517:71?140 (2012)
29. Wasserman, F.: The development of adipose tissue. Compr physiol Supplement 15: Handbook of Physiology, Adipose Tissue:87-100 (2011)

Index

acronyms, list of, xvii

dedication, v

foreword, vii

preface, ix

symbols, list of, xvii